A Quantitative Description of the Dynamics of Excitation and Inhibition in the Eye of *Limulus*

BRUCE W. KNIGHT, JUN-ICHI TOYODA, and
FREDERICK A. DODGE, Jr.

From The Rockefeller University, New York 10021

ABSTRACT By means of intracellular microelectrode techniques, we have measured the dynamics of the several processes which translate light stimulation into spike activity in the *Limulus* eye. The transductions from light to voltage and from voltage to spike rate, and the lateral inhibitory transduction from spike rate to voltage, we have characterized by transfer functions. We have checked the appropriateness of treating the eye as a system of linear transducers under our experimental conditions. The response of the eye to a large spot of light undergoing sine flicker has been correctly predicted.

1. INTRODUCTION

The faceted lateral eye of the horseshoe crab, *Limulus polyphemus*, exhibits many functional characteristics in common with the visual systems of more evolved creatures, including man. In this compound eye the relative accessibility of the nerve cells to the techniques of electrophysiology has led to a fairly detailed understanding of the actions of its components, and has made it a particularly attractive model system for the study of sensory neural function. This relatively simple visual organ performs three distinct processing steps upon signals arriving from the outside world. The first step is the translation of light intensity into intracellular voltage. The voltage in turn establishes the rate at which nerve impulses are sent to the brain. Third, the impulse rate is converted back into voltage, to perform the functions of neural inhibition. Here we will present detailed experimental measurements of the time-dependence of the several steps in signal processing which occur in the *Limulus* eye, and will then show how these results lead to a prediction of the time-dependent behavior of the eye as a whole.[1]

The voltage spikes, which travel down the *Limulus* optic nerve fibers toward

---

[1] A recent review article (Dodge, Shapley, and Knight, 1970) discusses this topic briefly.

the brain, originate in the eye near the soma of the neuron (eccentric cell). It was observed by MacNichol (1956) and by Fuortes (1959) that the steady-state spike rate is proportional to the degree of depolarization of the cell. Under conditions of normal functioning this depolarization is the combined effect of several different more peripheral causes. The action of light on the eye is to depolarize the eccentric cell, the result of an increase in membrane conductance that short-circuits the resting polarization of the cell (Tomita, 1956; Fuortes, 1959; Rushton, 1959). The basis of this conductance increase appears to be the superposition of numerous brief, discrete, conductance events which are triggered by absorption of photons (Yeandle, 1958; Fuortes and Yeandle, 1964), and which individually adapt to smaller size in brighter light (Adolph, 1964; Dodge, Knight, and Toyoda, 1968). Opposing the excitatory effect of light is *lateral inhibition* (Hartline, Wagner, and Ratliff, 1956) acting among neighboring eccentric cells. That lateral inhibition depends on the firing of spikes was demonstrated indirectly by quantitative analysis of the inhibitory interaction (Hartline and Ratliff, 1958), and directly by experiments in which inhibition was elicited by antidromic stimulation of the optic nerve (Tomita, 1958). Later, Tomita, Kikuchi, and Tanaka (1960), and Purple (1964; Purple and Dodge, 1965) demonstrated that antidromic inhibition resulted from a hyperpolarizing potential change associated with an increase in membrane conductance; thus lateral inhibition shows the usual features of a classical inhibitory postsynaptic potential. The lateral inhibitory interconnections have been identified anatomically (Hartline, Ratliff, and Miller, 1961), and detailed measurements have been made of the dependence of the inhibitory interaction upon the distance of separation between receptors (Barlow, 1967, 1969). Following the discharge of each spike an eccentric cell also shows a *self-inhibitory* hyperpolarization which is accompanied by a conductance increase, and displays the general features of an inhibitory postsynaptic potential (Stevens, 1964; Purple, 1964; Purple and Dodge, 1965, 1966).

Among the functional characteristics that the eye of *Limulus* and the human eye share are the following: (*a*) great sensitivity to *changes* in light intensity as compared to steady intensity level; (*b*) graded response to a wide range of light intensities (to a factor of about 10^7 in intensities for *Limulus*); (*c*) enhanced response to edges and contours. We note that the presence of self-inhibition should give rise to (*a*) above, the adaptation of the excitatory conductance should give rise to (*a*) and (*b*), and lateral inhibition to (*a*), (*b*), and (*c*). Several models, based on simple assumptions concerning the dynamics of the component processes within the eccentric cell, have yielded reasonable simulated responses to steps of input stimulation (Hartline et al., 1961; Stevens, 1964; Purple, 1964; Purple and Dodge, 1965, 1966; Lange, 1965; Lange, Hartline, and Ratliff, 1966). In this paper we present detailed experi-

mental characterizations of the dynamics of the one excitatory and the two inhibitory processes in the eccentric cell, and from these we predict the dynamics of the entire eye.

Fig. 1, which shows the response of a single fiber to incremental steps in light intensity (Ratliff, Hartline, and Miller, 1963), is a striking illustration of the sensitivity of the *Limulus* eye to changes in intensity. The great relative compression of response to time-independent intensity, shown in Fig. 1, makes the eye's high sensitivity to changes compatible with a wide range of input intensities.
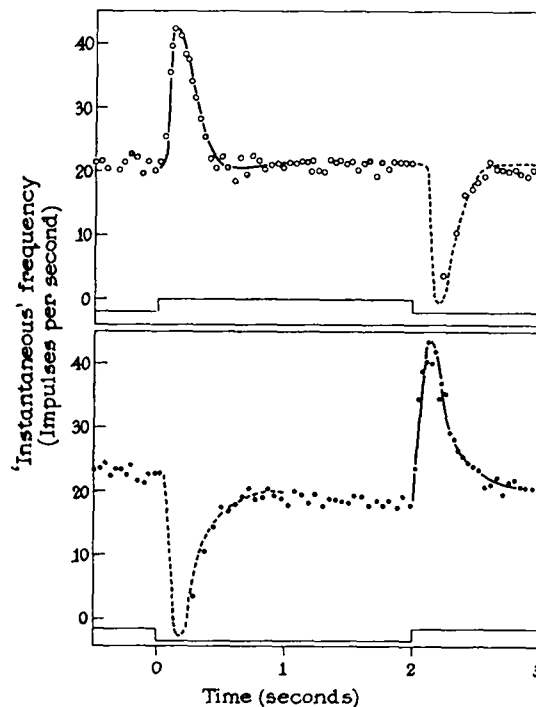

FIGURE 1. Response of the spike rate of an optically isolated eccentric cell to a step in light intensity. In each frame the solid line at "on" is fit to the points, and its reflection gives the dashed line at "off." Lower trace is light intensity. (From Ratliff et al., 1963). Log adapting $I = -0.26$; log I during increment $= 0.0$; log I during decrement $= -0.50$. *Figure reprinted by permission from Journal of the Optical Society of America. 1963. 53:110.*

A less obvious feature of Fig. 1 is crucial to the analysis that will follow. In both frames the response to an intensity decrement is the close mirror image of the response to the corresponding increment. This suggests that we are dealing with a so-called "time-invariant linear" system.

A time-invariant linear system has a property somewhat more general than that shown in Fig. 1. Namely, application of a superposition of individual inputs leads to the corresponding superposition of individual outputs, and the result is independent of the time of application. This is the principle of superposition, which we now assume for simplicity. A consequence of this property may be shown: a sine wave input necessarily leads to a sine wave output at the same frequency but generally with a different amplitude and at a different phase.

Now it is well-known that any physically realizable input can be expressed as a superposition of sine waves, each with its own amplitude and phase. (This is a form of the famous Fourier theorem.) This result, together with the principle of superposition, leads to the following very important conclusion.

Knowledge of the input-output amplitude ratio (amplitude gain) and the input-output phase shift, at all frequencies, completely specifies the input-output dynamics of a time-invariant linear system. This knowledge enables us to predict the system response to any arbitrary input.

2. METHODS

The excised *Limulus* lateral eye was split horizontally with a razor blade to expose the neural tissue behind the individual facets. One half-eye was mounted vertically (with beeswax) to form the fourth side of a three-sided moist chamber, with the exposed tissue facing upward. The chamber was filled with seawater, full enough to just cover the cut. A glass micropipette (3 molar KCl, 10–20 megohms) was lowered into an ommatidium by means of a micromanipulator and under visual control through a dissecting microscope. Electrical recording from the microelectrode was through a unity-gain amplifier with capacitance neutralization and a bridge circuit which permitted direct measurement of pipette and cell resistance and also allowed voltage recording while current was passed into the cell. The eye facets looked horizontally outward from the moist chamber, permitting light stimulation from a single optical fiber, 70 μ in diameter (American Optical Corp.), mounted on another micromanipulator. Earlier multifiber experiments demonstrated that light may be confined to a single facet in this way. The optical fiber was illuminated by a glow-modulator tube (Sylvania R 1131-C). The light intensity was controlled by modulating the repetition rate of 1 msec long light pulses, around a carrier frequency of 400 pulses per sec. Under these operating conditions, no appreciable nonlinear effects arise from the glow-modulator tube. The intensity range was chosen by the use of neutral density filters. Because the effective stimulus intensity was critically dependent on the alignment of the optical fiber to the axis of the ommatidium, we did not calibrate the light by any other method than the response of the eccentric cell. Maximum light intensity typically produced a steady-state firing of 30–40 spikes/sec in an optically isolated ommatidium. Previously reported techniques were used in the experiments in which single nerve fiber recordings were made (Hartline and Graham, 1932), and in those in which the optic nerve was stimulated antidromically (Tomita, 1958; Lange, 1965; Lange et al., 1966). All experiments were done at room temperature (19°–23°C).

In order to limit ourselves to a reasonably uniform population of cells, we accepted only definite eccentric cell recordings (spikes $\geq$ 30 mv). The advent of such an intracellular penetration is accompanied by an unmistakable fusillade of spike activity on the audio-monitor. The isolation of the excitatory process from spike activity was accomplished by the addition of tetrodotoxin to the seawater in the moist chamber.

An automatic timer gated the start of each experimental run and also the span of the light signal. Typically runs were spaced 100 sec apart, with the light on for 17

sec. This timing remained fixed for all runs on any given cell. Sinusoidal modulation was obtained from a function generator (Hewlett-Packard 3300A) whose frequency was set manually for each new run. A phase mark at the crest of each cycle was recorded from a second channel of the function generator.

The occurrence times of nerve spikes and phase marks, and the time course of the intracellular voltage, were recorded by a small computer (CDC 160-A) and stored in a Fortran-compatible format on digital tape. Event times were recorded in terms of the count of a crystal clock which incremented each 200 μsec. Records of the intracellular potential changes were made by feeding the voltage output of a monitoring oscilloscope (Tektronix 502A) to the computer through an analogue-digital converter. The oscilloscope output voltage was sampled every 200 μsec, and was averaged in the computer over 20 msec before storage on tape.

Fig. 2 shows direct graphical transcriptions of the data from individual runs. In the spike records the vertical coordinate is the "*instantaneous frequency*": the reciprocal of the time interval from the previous spike to the current spike. To a span of each record we have fit, by least squares, a combination of six time functions: a constant, a linear ramp, a cosine and a sine of the input frequency, and a cosine and a sine of twice the input frequency. The constant measures the mean level of the output and the ramp tells the drift of the preparation during a run. Cosine and sine of twice the input frequency measure "harmonic content," which is a check on whether the biological input-output system is responding linearly. The coefficients of cosine and sine at the input frequency are easily converted into amplitude gain and phase—the goal of these experiments. (This gain and phase information vs. frequency we will call the "frequency response" or "transfer function.") In Fig. 2 the least square fits have been superimposed on the raw data. This calculation of fitting coefficients may be regarded as a linear filter applied to the raw data. It proves to be a narrow-pass filter which passes the driving frequency undiminished, and has a bandwidth which is the reciprocal of the time span over which data are taken. This filter has a signal/noise discrimination superior to the familiar computer of average transients: it exploits the fact that a signal of known form lies beneath the noise.

In the experiments reported below, the sinusoidal modulation of the input signal had a peak-to-peak amplitude which was as much as 60% of the mean input signal. (See last frame of Fig. 2.) The second harmonic content of the output rarely exceeded 5% of the amplitude of the output fundamental. The largest harmonic distortions were concurrent with the largest output modulations. We were able, by reducing the input modulation, to spot-check the fact that gain amplitude and phase of the output fundamental were indeed independent of input modulation amplitude under our experimental conditions. This gave us some confidence in treating the *Limulus* eye as a linear system.
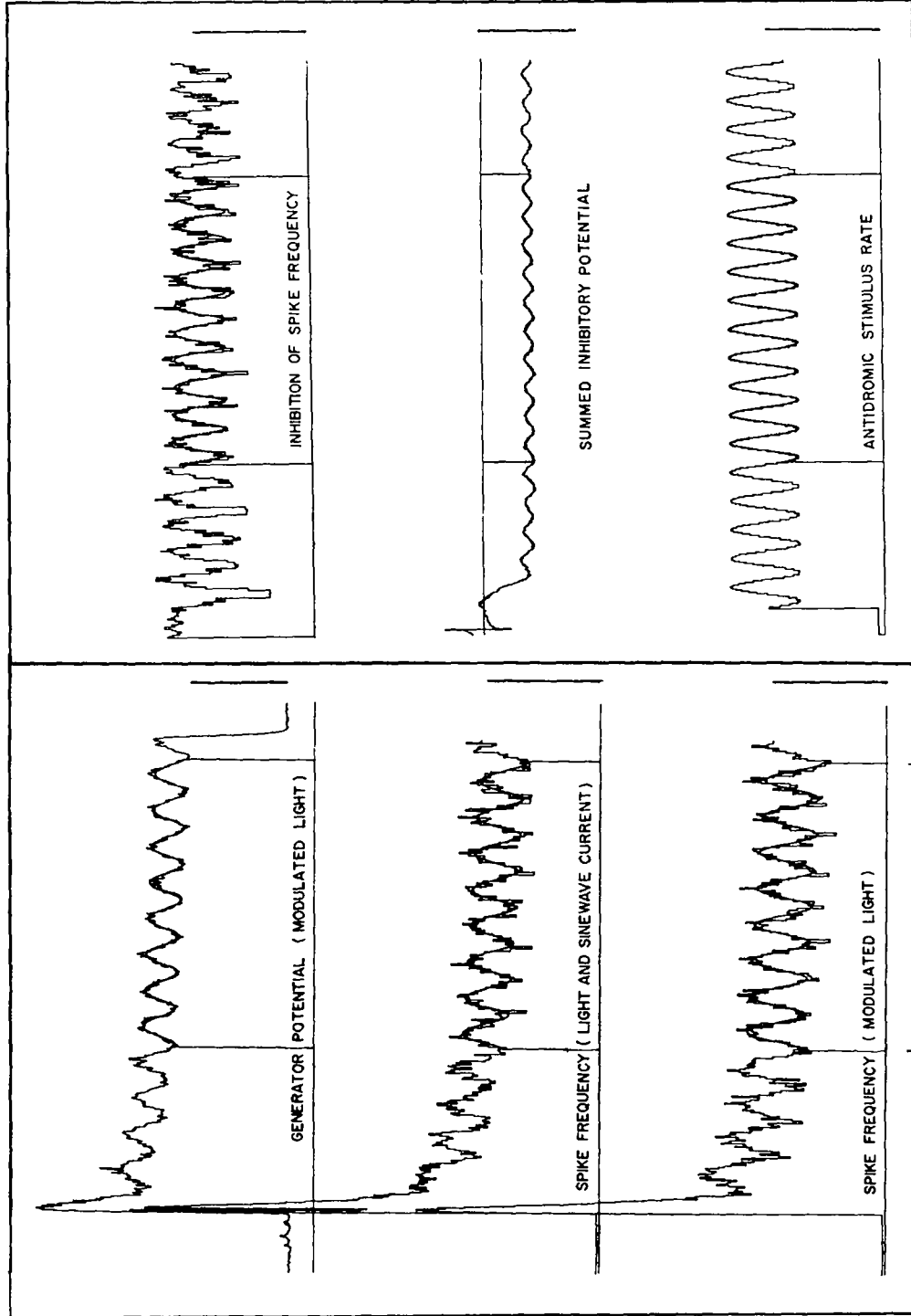
FIGURE 2.   Raw data for five transduced responses and a stimulus. Reading vertically the transductions are: light-to-voltage, voltage-to-spike rate, light-to-spike rate, inhibitory-spike rate-to-spike rate, inhibitory-spike rate-to-inhibitory voltage. The sixth frame gives the instantaneous spike rate of the antidromic inhibitory stimulus. Calibration, 10 mv for voltage records, 10 impulses/sec for spike rate records. Least squares fit in between vertical lines (see text).

In order to display these measurements (Figs. 3–5) we have normalized the amplitude to the value at zero frequency, which was calculated from the modulation depth of the stimulus and the slope of the steady-state stimulus-response relation. This normalization procedure is convenient because it uses only measurements of the incremental response. We can synthesize the empirical frequency response without taking explicit account of such complications as the threshold depolarization for spike firing and the variation of input resistance of the cell with ambient light intensity. Normalization factors for the several experiments are listed in Table I.

TABLE I

NORMALIZATION FACTORS FOR THE EMPIRICAL
FREQUENCY RESPONSE CURVES

Identifier	3/22/66 −0.3 log	4/29/66 −1.3 log	4/29/66 −3.0 log	9/23/66 −1.0 log	9/23/66 −2.6 log
Spike rate parameters (light to spikes)					
Unit amplitude,* sec^{-1}	1.5	1.2	1.2	1.3	1.3
Mean rate, sec^{-1}	17	27	14	35.5	18
Relative stimulus modulation‡	0.19	0.14	0.14	0.23	0.23
Peak-to-peak response at 1 Hz, sec^{-1}	15	10.1	6.2	12.4	8.6
Gains§ at 1 Hz	4.5	2.7	3.1	1.5	2.0
Generator potential parameters					
Unit amplitude,* mv	0.56	0.64	0.64	1.05	1.05
Mean value, mv	14.3	16.1	12.7	21.4	12.7
Relative stimulus modulation‡	0.38	0.28	0.28	0.40	0.40
Peak-to-peak response at 1 Hz, mv	2.05	1.52	1.18	3.64	3.18
Gain§ at 1 Hz	0.38	0.34	0.33	0.42	0.63

* Absolute modulation of response at zero frequency, calculated from slope of steady-state relation and stimulus modulation.

‡ Ratio of peak-to-peak modulation of light intensity to the mean value.

§ Defined as (peak-to-peak response/mean response)/(peak-to-peak stimulus/mean stimulus).

3. RESULTS

Dynamics of the Single Photoreceptor

For convenience, we will refer to any collection of cellular machinery, which modifies the form of a signal, as a "transducer"; the modifying process will be called "transduction." The behavior of the *Limulus* eye arises from three types of neural transducers, which we have isolated experimentally and whose frequency responses we have measured: (a) the transduction of light intensity to intracellular voltage, (b) the transduction from input voltage to spiking rate (this includes self-inhibition), and (c) the lateral inhibitory transduction from spiking rate back into voltage.

In the left frame of Fig. 3 the open circles show the frequency response of the intracellular generator potential, of a single illuminated ommatidium, to sinusoidally flickering light. (See also Pinter, 1966; Dodge et al., 1968.) Nerve spike activity has been abolished by the application of tetrodotoxin.

The frequency response of spike rate, in response to driving voltage, is shown for the same cell by the solid circles in the left frame of Fig. 3. Mean spike rate was maintained by steady light on the receptor, while sinusoidal voltage modulation was achieved by driving a sinusoidal current through the intracellular micropipette.

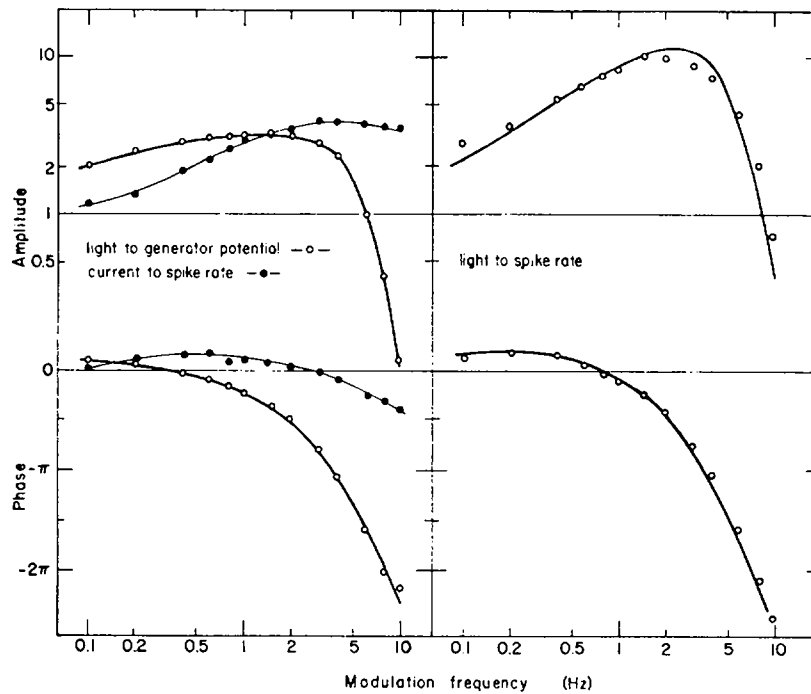Both frequency responses show the general features of a transducer which applies a "sluggish gain control" to input signals. The amplitude gain first

Modulation frequency (Hz)

FIGURE 3. Data of 9/23/66 -2.6 log. Left frame, amplitude and phase of frequency response of component transductions, light-to-voltage (open circles) and voltage-to-spike rate (solid circles). Right frame, frequency response of total transduction, light-to-spike rate. Data points from direct measurement, solid curves predicted from left frame.

increases with frequency, as the gain control becomes less able to follow the input signal. Since such a gain control still will be reducing the output signal at the moment when the input sine wave reaches its crest, there will be a low-frequency phase lead. Eventual high-frequency cutoff and phase lag may be anticipated on very general grounds: any real transducer will have a time-resolution limitation; and the time necessary for internal processing will impose a lag between input cause and output effect as that limitation is approached.

Under circumstances of normal operation the sinusoidal output of the light-to-voltage transducer would be the sinusoidal input to the voltage-to-spike

rate transducer. Clearly the amplitude gain of the combination should be the product of the amplitude gains of its two components, and the corresponding phase shift should be the algebraic sum of the two component phase shifts. The indicated multiplication and addition have been done, and the results appear as the solid curves in the right frame of Fig. 3. The direct experiment
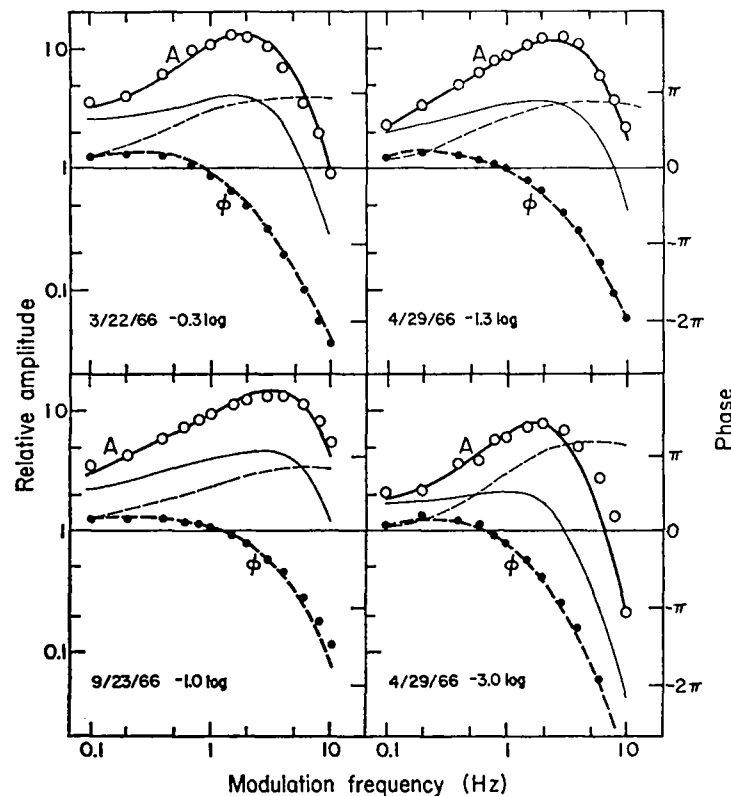

FIGURE 4. Four more predictions of light-to-spike rate frequency response compared with direct measurement (open and closed circles). Thin solid curves, light-to-voltage. Thin dashed curves, voltage-to-spike rate. Heavy curves, light-to-spike rate predicted. Phase data of component transductions are not shown.

has also been done on the same cell: the frequency response of the firing rate to a sinusoidally flickering light has been measured, and is shown by the open circles in the same illustration.

Fig. 4 summarizes the results of four similar experiments. Prediction and measurement are in general agreement in all cases, and show no systematic discrepancies. Thus, by treating the two transducers as time-invariant linear systems, we have correctly predicted their combined effect.

The outcome of a voltage-to-spike rate experiment may be summarized in terms of

three parameters: the mean firing rate, the self-inhibitory time constant, and the self-inhibitory strength coefficient. The latter two parameters are evaluated by fitting equation (d) (footnote to theoretical section) to the data. The results obtained from 12 *Limulus* eyes are summarized in Table II.

Dynamics of Lateral Inhibition

Under normal operating conditions the frequency response of the lateral inhibitory potential cannot be measured directly. The inhibitory potential is

TABLE II
ESTIMATES OF SELF-INHIBITION PARAMETERS

Identifier	L	Spike rate	Time constant	Self-inhibitory coefficient
		sec^{-1}	sec	
3/16/66	i	17	0.75	1.8
3/22/66	−0.3	20	0.70	2.9
4/5/66	i	15	0.45	3.5
4/29/66	−3.0	20	0.40	4.0
	−1.3	31	(0.6)*	2.5
9/23/66	−2.6	19	0.50	3.0
	−1.0	34	(0.6)*	2.5
3/30/67	a	15	0.50	3.8
4/7/67	a	16	0.55	5.0
4/11/67	a	19	0.50	4.0
4/14/67	a	20	0.80	3.5
4/17/67	a	20	0.55	2.5
4/24/67	a	19	0.60	3.2
5/2/67	a	15	0.45	6.0

L, Background light intensity in terms of logarithm of attenuation of standard source, except:

    i, Modulation superimposed on depolarizing current.

    a, Bright steady light (−0 log) but spike rate diminished by antidromic inhibition.

* Data not fit well by single time constant; estimate given is approximate fit to amplitude at half-maximal value.

written over by the spike activity of the postsynaptic cell. However, an indirect measurement was possible. First, we measured the frequency response of the voltage-to-spike rate transducer as discussed above, using an eye whose optic nerve was prepared for antidromic stimulation of the whole nerve. (The nerve fiber to the impaled cell was severed to prevent antidromic invasion.) Then, with steady light on the recording ommatidium and with no stimulating current passed through the microelectrode, we antidromically stimulated the optic nerve at a rate upon which we imposed a sinusoidal modulation (see last frame of Fig. 2). The resulting modulation in the spike activity of the impaled cell yielded the total transduction from neighbors to test unit: spike rate-to-voltage-to-spike rate. Reversing the earlier procedure,

we respectively divided and subtracted these results by the amplitude and phase of the voltage-to-spike rate transduction, to recover the frequency response of the lateral inhibitory synapse. The results for three eyes are shown in Fig. 5.

By altering the intracellular conditions of the impaled eccentric cell, the lateral inhibitory frequency response may be observed directly. The eye was
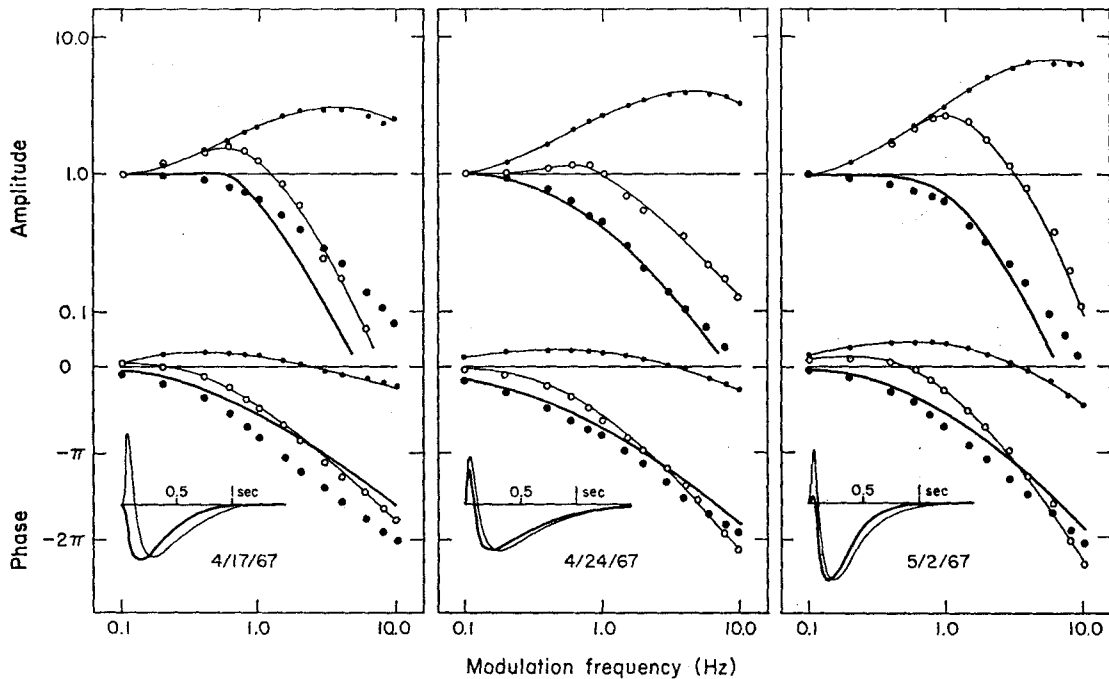

FIGURE 5.   Lateral inhibitory transduction. Small solid circles, voltage-to-spike rate. Open circles, inhibitory-spike rate-to-spike rate. Heavy line, deduced frequency response for inhibitory-spike rate–to–inhibitory-potential transduction in presence of ongoing spike activity in postsynaptic cell. Heavy circles, directly observed inhibitory-spike rate–to–inhibitory-potential in hyperpolarized and quiet cell. Insert, Postsynaptic impulse response predicted by Fourier analysis. Heavy line, active cell. Thin line, hyperpolarized cell.

put in darkness and the cell hyperpolarized to the point at which spike activity ceased. Then the same antidromic stimulation yielded a postsynaptic voltage measurable through the microelectrode. For the three cases of Fig. 5 the directly measured frequency response is shown with solid circles. There is approximate agreement with the indirect measurement, though the departures are systematic.

The insets in Fig. 5 may cast some light on the discrepancy. In the introduction it was mentioned that the frequency response may be used to calculate the response to an arbitrary input. We have used the frequency response
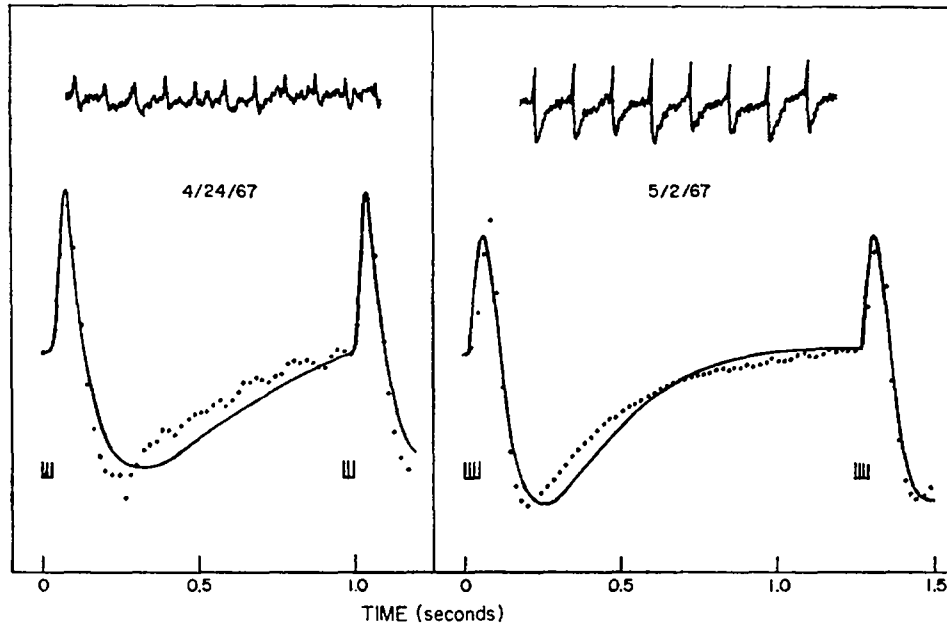
FIGURE 6.   Comparison of impulse response predicted by Fourier analysis (line) with averaged transient observed directly (solid circles). Insert shows several cycles of the raw impulse response data. The "impulse" for the left frame consisted of three antidromic whole nerve stimuli spaced at intervals of about 10 msec. In the right frame four such stimuli were used.
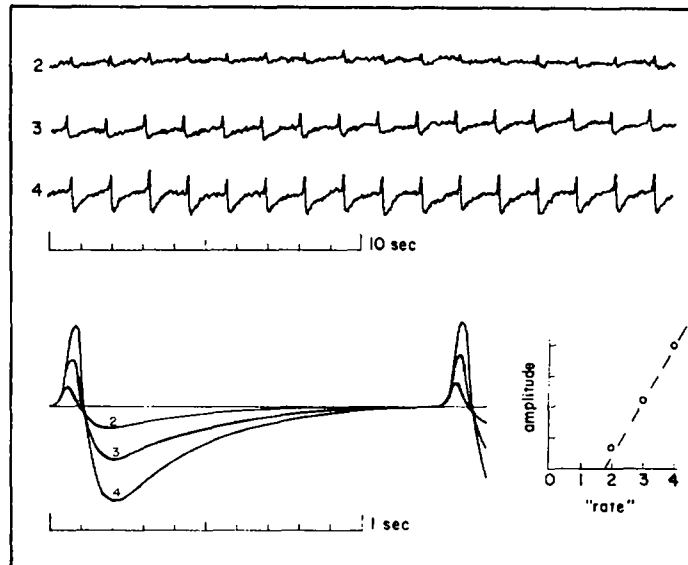

FIGURE 7.   Facilitation phenomenon. The averaged postsynaptic voltage response to two, three, and four nerve impulses spaced about 10 msec apart. Beyond threshold the response is linear.

to calculate the response to a brief impulsive input; the result should be the time course of the unit inhibitory postsynaptic potential. In five of the six cases there is a remarkable brief depolarization before the onset of the main inhibitory potential. In all three cells the depolarizing surge is more pronounced when the cell is in the more hyperpolarized condition. This observation is consistent with the notion that the brief depolarization results from an additional postsynaptic permeability change (Kandel and Wachtel, 1968) whose equilibrium potential is positive to the operating voltages within the cell. (By the same token, the hyperpolarizing part of the postsynaptic response is more pronounced when the cell is depolarized. This is not evident in Fig. 5 because the transfer functions have been normalized to unity at zero frequency.)

In the hyperpolarized and quiet cell, the postsynaptic impulse response predicted from frequency information may be compared to that measured directly. The result is shown in Fig. 6. The degree of agreement may be regarded as validation for our treating the lateral inhibitory synapse as a time-invariant linear transducer.

In Fig. 7 are shown the mean postsynaptic voltage responses to two through four closely spaced antidromic impulses. Apparently two stimulating impulses are necessary to facilitate the synapse, which then responds linearly to further increments in input.

4. THEORETICAL

Finally, we use these results to predict the behavior of the entire eye. The time-independent firing rates of the *Limulus* eccentric cells are known to satisfy the Hartline-Ratliff equations (Hartline and Ratliff, 1958):

$$r_m = \epsilon_m - K r_m - \sum_{n \neq m} k_{mn} r_n , \tag{1}$$

presented here in a form which includes self-inhibition explicitly. Here r_m is the firing rate of the mth ommatidium, K is its self-inhibitory coefficient, ϵ_m is its excitatory receptor potential expressed in appropriate units, and k_{mn} are the lateral inhibitory coefficients linking it to other ommatidia. Small threshold corrections have been discarded. While the success of these equations is empirical, the three right-hand terms may be interpreted as the three contributions to the intracellular voltage at the site of voltage-to-spike rate transduction. This observation leads to the immediate frequency-dependent generalization of equation 1.

From electrical and control system design it is well-known that a sinusoidally modulated variable may be represented by a complex number fixed in amplitude but advancing in phase at a rate which yields the modulation frequency. The effect of a linear transducer upon that variable is to multiply

it by a complex number (the "transfer function") whose amplitude and phase
are the amplitude gain and phase of the transducer's frequency response at
that frequency. This shorthand scheme is useful because it yields correct re-
sults not only for the application of consecutive transductions but also for the
addition of several out-of-phase signals. That is exactly what is required to
generalize equation 1.

Following this scheme, if I is the modulation in light intensity, then the
modulation in receptor potential is given by

$$\epsilon_m = G(f)I \qquad (2)$$

where the transfer function $G(f)$ is the complex number whose amplitude and
phase are given by the frequency response in Fig. 3 (left frame, open circles),
evaluated at the modulation frequency f. The generalization of equation 1
is similarly

$$r_m = \epsilon_m - KT_s(f)r_m - T_l(f) \sum_{n \neq m} k_{mn}r_n . \qquad (3)$$

Here T_s and T_l are the self-inhibitory and lateral inhibitory transfer functions
so scaled that they are unity when $f = 0$. The amplitude and phase of the
lateral inhibitory $T_l(f)$ are given by the spike rate–to–voltage curves of
Fig. 5. Fig. 3 (solid circles) determines the form of $T_s(f)$.[2] Now given the ϵ_m

---

[2] Dropping the summation term in (3) easily leads to the determining equation

$$KT_s(f) = \frac{1}{(r/\epsilon)} - 1 \qquad (a)$$

where (r/ϵ) is the solid circle frequency response of Fig. 3.

There is a slight approximation in equation (3) because the frequency-dependent transduction
effects of the voltage-to-spike rate converter have been ignored. It is easily shown for an exponential
inhibitory postsynaptic potential with decrement time τ that

$$T_s = \frac{1}{1 + i\tau\omega} \qquad (b)$$

where $\omega = 2\pi f$, whence (a) gives

$$r/\epsilon = \frac{1}{1 + KT_s} = \frac{1}{1 + K\dfrac{1}{1 + i\tau\omega}} \qquad (c)$$

which fits the data of Fig. 3 (and similar Limulus data) fairly well. (This result is equivalent to the
model of Stevens, 1964.) If one assumes that the spikes arise from an integrating voltage-to-fre-
quency converter, an unpleasant perturbation calculation yields the exact transfer function

$$r/\epsilon = \left(\frac{1 - e^{-i\omega/\nu}}{i\omega/\nu}\right) \Big/ \left(1 + K\left[1 - \frac{(1/\tau\nu)(1 - e^{-i\omega/\nu})}{(e^{1/\tau\nu} - 1)(1 - e^{-(1/\tau+i\omega)/\nu})}\right]\right) \qquad (d)$$

where ν is the mean spike rate. Equation (c) is retrieved in the limit $\omega/\nu \rightarrow 0$ (Terzuolo, 1969,
see pp. 65–69). However, (d) shows a high-frequency amplitude cutoff and phase lag (which (c)

(from equation 2), the equations (3) are in the form of a set of linear simultaneous equations, which at each modulation frequency can be solved for the r_m.

We have tried to use equations 2 and 3 with our data to predict the outcome of another experiment (Ratliff, Knight, Toyoda, and Hartline, 1967), in which first a single ommatidium, and then a circular cluster of 20 ommatidia were stimulated by a flickering light. The firing rate modulation of the central fiber was determined by a single fiber recording. For the calculation we used
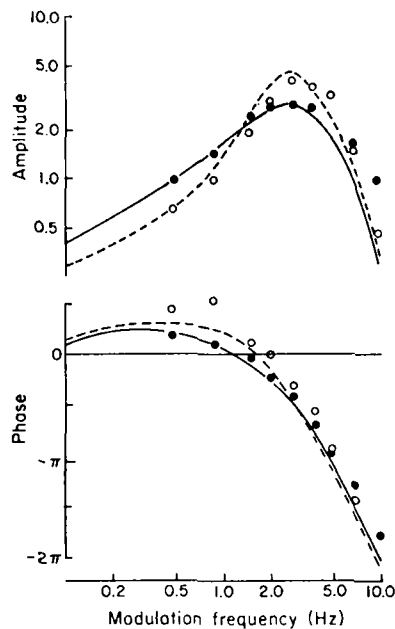

FIGURE 8. Theoretical and observed light-to-spike rate frequency response for a single ommatidium and for the central member of a cluster of 19 interacting ommatidia. Amplitude is given in sec^{-1} peak-to-peak. Mean rate was 25/sec for solid circles and 20/sec for open circles.

the data from two comparable ommatidia: the generator transfer function given in the upper right frame of Fig. 4, and the lateral inhibitory transfer function given in the middle frame of Fig. 5. We used the commonly observed self-inhibitory coefficient value of $K = 3$ and the spatial distribution of lateral inhibition given by Barlow (1969).

A hexagonal array of 19 ommatidia has been assumed. Because there are two axes of symmetry in the Barlow inhibitory distribution, only seven of these ommatidia are mathematically inequivalent. Seven simultaneous equations similar to the set (3) result, and have been solved for a range of frequencies. The frequency response thus obtained for the central ommatidium has been multiplied by the light-to-voltage transfer function. In Fig. 8 this

does not) and in fact fits very well to most of our *Limulus* voltage-to-spike rate transfer function experiments. The predictions which follow utilize the theoretical embellishments which led to (d). However, the difference in result from that of the simpler approximate relation (3) is slight.

theoretical result is compared with the experiment. One remaining parameter, which fixes the scale of the over-all amplitude gain, has been fit by placing the "large spot" theoretical amplitude line through the corresponding data point at 0.5 hz. In the final result, the discrepancies between theory and experiment are small compared to individual variations among ommatidia seen in Figs. 4 and 5.

5. CONCLUSIONS

Over a reasonable range of stimulus illumination, the eye of *Limulus* responds as a linear transducer.

Within the eye three component transductions may be isolated and studied individually. These are the transductions from light to voltage, from voltage-to-spike rate, and the lateral inhibitory transduction from spike rate back to voltage. These are all linear transductions and their individual frequency responses may be measured.

The transductions from light to voltage and from voltage-to-spike rate both have frequency responses whose general form is that of a sluggish gain control.

The lateral inhibitory transduction from spike rate to voltage corresponds to a unit postsynaptic potential which is briefly excitatory before its more pronounced inhibitory phase sets in.

These component frequency responses may be utilized in a time-dependent generalization of the Hartline-Ratliff equations. The over-all dynamic response of an interacting group of ommatidia, to sinusoidal flicker, is predicted properly.

REFERENCES

ADOLPH, A. R. 1964. Spontaneous slow potential fluctuations in the *Limulus* photoreceptor. *J. Gen. Physiol.* 48:297.

BARLOW, R. B., JR. 1967. Inhibitory Fields in the *Limulus* Lateral Eye. Thesis. The Rockefeller University. New York.

BARLOW, R. B., JR. 1969. Inhibitory fields in the *Limulus* lateral eye. *J. Gen. Physiol.* 54:383.

DODGE, F. A., B. W. KNIGHT, and J. TOYODA. 1968. Voltage noise in Limulus visual cells. *Science (Washington).* 160:88.

DODGE, F. A., R. M. SHAPLEY, and B. W. KNIGHT. 1970. Linear systems analysis of the *Limulus* retina. *Behav. Sci.* 15:24.

FUORTES, M. G. F. 1959. Initiation of impulses in visual cells of *Limulus. J. Physiol. (London).* 148:14.

FUORTES, M. G. F., and S. YEANDLE. 1964. Probability of occurrence of discrete potential waves in the eye of *Limulus. J. Gen. Physiol.* 47:443.

HARTLINE, H. K., and C. H. GRAHAM. 1932. Nerve impulses from single receptors in the eye. *J. Cell. Comp. Physiol.* 1:277.

HARTLINE, H. K., and F. RATLIFF. 1958. Spatial summation of inhibitory influences in the eye of *Limulus*, and the mutual interaction of receptor units. *J. Gen. Physiol.* 41:1049.

HARTLINE, H. K., F. RATLIFF, and W. H. MILLER. 1961. Inhibitory interaction in the retina, and its significance in vision. *In* Nervous Inhibition. E. Florey, editor. Pergamon Press, New York. 241.

HARTLINE, H. K., H. G. WAGNER, and F. RATLIFF. 1956. Inhibition in the eye of *Limulus*. *J. Gen. Physiol.* 39:651.

KANDEL, E. R., and H. WACHTEL. 1968. The functional organization of neural aggregates in *Aplysia*. *In* Physiological and Biochemical Aspects of Nervous Integration. F. D. Carlson, editor. Prentice-Hall, Inc., Englewood Cliffs, N. J. 17.

LANGE, D. 1965. Dynamics of Inhibitory Interaction in the Eye of *Limulus*: Experimental and Theoretical Studies. Thesis. The Rockefeller University. New York.

LANGE, D., H. K. HARTLINE, and F. RATLIFF. 1966 *a*. Inhibitory interaction in the retina: techniques of experimental and theoretical analysis. *Ann. N.Y. Acad. Sci.* 128:955.

LANGE, D., H. K. HARTLINE, and F. RATLIFF. 1966 *b*. Dynamics of lateral inhibition in the compound eye of *Limulus*. II. *In* The Functional Organization of the Compound Eye. C. G. Bernhard, editor. Pergamon Press, Oxford. 425.

MacNICHOL, E. F., JR. 1956. Visual receptors as biological transducers. *In* Molecular Structure and Functional Activity of Nerve Cells. *Am. Inst. Biol. Sci. Publ. No. 1.* 34–53.

PINTER, R. B. 1966. Sinusoidal and delta function responses of visual cells of the *Limulus* eye. *J. Gen. Physiol.* 49:565.

PURPLE, R. L. 1964. The Integration of Excitatory and Inhibitory Influences in the Eccentric Cell in the Eye of *Limulus*. Thesis. The Rockefeller University. New York.

PURPLE, R. L., and F. A. DODGE, JR. 1965. Interaction of excitation and inhibition in the eccentric cell in the eye of *Limulus*. *Cold Spring Harbor Symp. Quant. Biol.* 30:529.

PURPLE, R. L., and F. A. DODGE, JR. 1966. Self inhibition in the eye of *Limulus*. *In* The Functional Organization of the Compound Eye. C. G. Bernhard, editor. Pergamon Press, Oxford. 451.

RATLIFF, F., H. K. HARTLINE, and W. H. MILLER. 1963. Spatial and temporal aspects of retinal inhibitory interaction. *J. Opt. Soc. Amer.* 53:110.

RATLIFF, F., B. W. KNIGHT, J. TOYODA, and H. K. HARTLINE. 1967. Enhancement of flicker by lateral inhibition. *Science (Washington).* 158:392.

RUSHTON, W. A. H. 1959. A theoretical treatment of Fuortes' observations upon eccentric cell activity in *Limulus*. *J. Physiol. (London).* 148:29.

STEVENS, C. F. 1964. A Quantitative Theory of Neural Interactions: Theoretical and Experimental Investigations. Thesis. The Rockefeller University. New York.

TERZUOLO, C. A., editor. 1969. Systems Analysis in Neurophysiology. Proceedings of Conference on Systems Analysis Approach to Neurophysiological Problems. University of Minnesota, Minn.

TOMITA, T. 1956. The nature of action potentials in the lateral eye of the horseshoe crab as revealed by simultaneous intra- and extracellular recording. *Jap. J. Physiol.* 6:327.

TOMITA, T. 1958. Mechanisms of lateral inhibition in the eye of *Limulus*. *J. Neurophysiol.* 21:419.

TOMITA, T., R. KIKUCHI, and I. TANAKA. 1960. Excitation and inhibition in lateral eye of horseshoe crab. *In* Electrical Activity of Single Cells. Y. Katsuki, editor. Igaku-shoin, Ltd., Tokyo, 11.

YEANDLE, S. 1958. Electrophysiology of the visual system-discussion. *Am. J. Ophthalmol.* 46:82.